High Affinity RNase S-Peptide Variants Obtained by Phage Display Have a Novel "Hot-Spot" of Binding Energy

John J. Dwyer,[‡] Mary A. Dwyer,[§] and Anthony A. Kossiakoff*

Department of Biochemistry and Molecular Biology, Institute for Biophysical Dynamics, University of Chicago, 920 East 58th Street, Chicago, Illinois 60637

Received August 21, 2001

ABSTRACT: Using phage display mutagenesis, high affinity variants of RNase S-peptide were produced that bind to RNase S-protein over 100-fold more tightly than the wild type S-peptide. The S-peptide:S-protein interface was further characterized using "biased" phage display libraries, where each targeted residue was constrained to be either polar or nonpolar. The use of these tailored libraries placed constraints on the type of interactions present during affinity maturation process and allowed more amino acids to be randomized simultaneously. These results, in conjunction with kinetic association and dissociation constants determined by surface plasmon resonance (SPR), highlight the role of a single mutation (A5W) in increasing S-peptide binding affinity. High affinity S-peptide variants were only identified when tryptophan was present in the phage display library at position 5, suggesting that this residue is a "hot-spot" of binding energy in the high affinity variants. Analysis of SPR data in the presence of denaturant suggests that the increased affinity is a result of increased hydrophobic interactions in the transition state rather than a stabilization of helical structure.

Molecular recognition is a fundamental element in essentially all biological processes. An understanding of the extraordinary variety and complexity inherent in molecular recognition events has been developed through studies combining structural and mutagenesis approaches. However, the key details of the interplay between the effects of enthalpic and entropic factors that define the binding properties at contact interfaces are not well understood and currently are the subject of intense investigation (for a review, see ref *1*).

Approaches that attempt to predict the overall binding interaction energy by assigning specific values to a hydrogen bond and unit of buried hydrophobic surface area have not been very successful for most types of protein−protein interactions. It is clear, for instance, that not every hydrogen bond contributes equally to a binding energy. In fact, most interactions are context dependent with the associated binding energy in a number of protein−protein systems being governed within the broad contact surface by a few key contact residues called binding "hot-spots" (*2*−*5*).

The binding "hot-spot" concept evolved from the seminal work of Wells and colleagues through their study of the binding energetics between human growth hormone and growth hormone receptor (*2*, *3*). Although this example has led to several new fundamental insights into the nature of protein−protein interactions, many issues remain unresolved. This results from the fact that such interfaces involve extremely large and complex surfaces [∼30 residues and extensive conformational change (*6*)]. To simplify the scope of the problem, we have chosen to study the interaction involving two independent folding domains of RNase S. This system limits the number of variables in the analysis but contains many of the same basic protein−protein elements as in the more complicated interfaces. Thus, it offers both a versatile and practical model to study the character of macromolecular interactions.

Although site-directed mutagenesis has proven to be a very powerful approach to investigate issues involving protein−protein interactions, it is highly limited in its ability to evaluate the type of energetic clustering embodied in phenomena like "hot-spot" binding. For instance, it is technically daunting to test an adequate set of combinations of mutations to assess the structural and contextual origins of the concentration effect in the binding "hot-spot". However, another technique, known as phage display mutagenesis, holds much promise (*7*−*9*). This technique is particularly powerful in that it allows for simultaneous amino acid changes among a number of targeted sites. Thus, it has the potential to evaluate synergistic relationships among several residues. The idea of directed evolution, that is, trying all combinations simultaneously at all functionally sensitive sites is a more inclusive approach than intellectually driven site-directed mutagenesis approaches that are much more limited in scope. Furthermore, the phage display approach has been found, in a process termed "affinity maturation", to be able to evolve new binding solutions having fundamentally different stereochemical and physicochemical properties compared to those of the original interaction.

In this report, we use RNase S as a model system to explore the redistribution of binding energy within the S-peptide:S-protein[1] interface after affinity maturation using phage display mutagenesis. RNase S is a modified enzyme

* To whom correspondence should be addressed. Phone: (773) 702-9257. Fax: (773) 834−2777. E-mail: koss@cummings.uchicago.edu.

[‡] Present address: Trimeris, Inc., Department of Biophysical Chemistry, 4727 University Dr., Durham NC 27707.

[§] Present address: Duke University Medical Center, Department of Biochemistry, Durham NC 27710.

10.1021/bi011703b CCC: $20.00 © 2001 American Chemical Society
Published on Web 10/20/2001

derived from the enzymatic cleavage of RNase A by subtilisin. It is active and is made up of two weakly associating fragments: the S-peptide (residues 1−20) and S-protein (residues 21−124). The protein−protein contact surface is along the interior face of the S-peptide α-helix and contains essential residues of the active site of the enzyme. RNase S has been studied extensively as a model system for molecular recognition (*10*), protein folding (*11*−*13*), and structure−function analysis (*14*). Extensive structural information is also available (*15*, *16*).

Since residues 3 through 13 of S-peptide must adopt a helical conformation for proper binding and activity, side chains that are important for binding have conformational constraints. Importantly, the relatively weak binding between the S-peptide and S-protein fragments is in a range where structure−function analysis by phage display mutagenesis is most powerful. The primary goals of this work were to establish which residues of S-peptide contribute most to the interaction with S-protein and to identify high affinity variants of S-peptide using phage display. S-peptide binding to S-protein was optimized using standard phage display libraries, as well as novel "biased" libraries in which specific residues were constrained to be either polar or nonpolar (*17*). Interestingly, it was found that changing just three residues resulted in a variant that bound 110-fold tighter than wild type. The use of biased libraries also demonstrated how alternative, high affinity variants could not be found without the presence of tryptophan at position 5.

Alanine scans of S-peptide and a high affinity variant, sequence comparisons from the phage sorting experiments, and differences in binding affinity were all used to identify the changes in the energy distribution after phage display optimization. After affinity maturation of S-peptide, a new "hot spot" of binding energy was found that did not appear to alter the importance of other contact residues. It is also shown that the use of biased phage display libraries offers the potential to control the type of interaction available in the optimization process, while allowing a larger subset of interface residues to be included in the library. Directed evolution using these libraries resulted in alternative solutions that would not have been easily identified using standard phage display libraries, and certainly not by site-directed mutagenesis approaches. The implications of these results on recognition and folding of S-peptide are also discussed.

EXPERIMENTAL PROCEDURES

Phage Display. Monovalent phage display libraries were constructed by expressing S-peptide variants as N-terminal extensions of the phage M13 coat protein, geneIII. These peptides were separated from the geneIII sequence by a Gly−Gly−Ser−Gly−Gly−Ser linker. This linker provides orientational flexibility to the expressed peptide, as well as spacing it away from the body of the phage to prevent indirect binding artifacts. For general reviews of phage display, see refs *7*−*9*, *18*.

[1] Abbreviations: S-peptide: a fragment of RNase A consisting of residues 1−19; S-protein: a fragment of RNase A consisting of residues 20−124; RNase S: the noncovalent complex of S-peptide and S-protein; MOI: multiple of infectivity; SPR: surface plasmon resonance; BSA: bovine serum albumin; PEG: poly(ethylene glycol); PBS: phosphate buffered saline; RU: resonance units.

Table 1: Codons and Library Parameters for Biasing Positions in a Phage Display library[a]

name	codon	amino acids obtained	no. codons	library size needed	max no. residues
polar	VRS	H,Q,N,K,D,E,R,S,G	12	2×10^9	8
nonpolar	NYS	K,L,S,P,M,I,T,V,A	16	1×10^9	7
aromatic	TNS	F,L,S,Y,stop,C,W	8	5×10^8	9
full randomization	NNS	all	32	1×10^9	5

[a] Characteristics of phage libraries biasing amino acids to polar, nonpolar, aromatic, nonaromatic, and nonbasic residues (*17*). For each type of biased residue, the represented codon, amino acids, and number of codons are listed in the above table. The nomenclature for these codons is as follows: N = G + A + T + C; V = A + C + G; Y = C + T; R = A + G; S = C+ G. Codon base wobbles are synthesized using deoxynucleotide mixtures as follows: 4 way- 25% each; 3 way- 33% each; 2 way- 50% each. For each biased library type, the maximum number of randomized residues is determined based on statistical calculations for total representation (4(no. codons)^n) where n is the number of randomized residues (*9*) and current electroporation limits (1×10^{10} independent transformants/ library). For biased libraries, the number of required transformants (library size) for complete representation are given as well as the maximum number of residues of that type that can be simultaneously mutated while ensuring total representation.

The targeted residues for mutagenesis were randomized using the NNS strategy that gives full coverage of all 20 possible amino acids (Table 1). Libraries of $\sim 2 \times 10^{10}$ transformants were prepared (Sachdev Sidhu, personal communication) and were screened by coating S-protein (Sigma) to 96-well plates (Falcon Maxisorb) at 20 μg/mL, blocking S-protein wells and control wells (no S-protein) with BSA, and incubating phage (diluted 1:10 in binding buffer) for 1 h. The binding buffer consisted of 50 mM KOAc, pH 5.5, 10 mM $CaCl_2$, 10 mM $MgCl_2$, and 150 mM NaCl. Wells were washed 10 times with buffer, and specifically bound phage was eluted with 0.2 N glycine (pH 2.2) and neutralized with 1 M Tris base to a final pH of ~8.0. Phage were propagated in 25 mL of 2YT media containing 8 μg/mL chloramphenicol plus VCS-M13 helper phage (Stratagene) at 10 MOI. Overnight cultures were harvested by pelleting the cells and adding 1/5 volume 20% PEG/2.5 M NaCl to the supernatant to precipitate the phage. Phage pellets were resuspended in 1 mL of PBS and stored at 4° until use. Enrichment was monitored by infecting mid-log phase E. coli (XL1-blue) with eluted phage (serially diluted) from S-protein and control wells and plating the culture out on selective media.

Construction of Biased Phage Display Libraries. Biased phage display libraries were constructed by using standard wobble codes described in Table 1 (*17*). These differ from the conventional NNS codon used in the fully randomized library. The VRS codon was used at each position targeted in the polar biased library. The nonpolar based biased library used a combination of codons derived from the NYS library and the TNS library. In a NNS based phage display library between $2(32)^n$ and $5(32)^n$ (n = number of residues mutated) independent transformants are required to ensure a complete library (*9*). Currently, library sizes of 10^{10} transformants can be achieved, and so the NNS library can theoretically represent all possible combinations of amino acids at five or six positions. Significantly more positions can be targeted in the biased phage display libraries because of the lower number of possible base combinations (Table 1).

After several rounds of binding selection, 20−30 individual clones were isolated and sequenced. Standard devia-

tions from the expected frequency were calculated by the following equation (*18*)

$$\sigma_n = [P_e(1 - P_e)/n]^{1/2} \quad (1)$$

where n is the number of clones sequenced, and P_e is the expected probability based on the number of codons for each amino acid. Note that the reported significance score, $(P_f - P_e)/\sigma_n$, where P_f is the fractional occurrence observed for a given residue, will be generally much lower than the corresponding score for NNS libraries, because the expected frequency (P_e) increases as the number of different amino acids in the library decreases.

The "soft-randomized" library was constructed by designing oligonucleotide primers that contained a 70:10:10:10 mixture of bases (70% of the wild-type base and 10% of the other three bases) for each of the 19 S-peptide residues. For each residue in the library, this mixture produces a mutation frequency of about 50% (*19*).

ELISA Alanine Scanning. The relative contribution to binding of each S-peptide residue along the interface was determined by expressing alanine mutants of S-peptide as fusions to geneIII. The relative affinities were estimated by normalizing the phage titers of each mutant, serially diluting the phage 1:2, and binding to a 96-well plate coated with S-protein under the same conditions as for phage sorting. After a washing step, a mouse anti-M13 phage monoclonal antibody conjugated to horseradish peroxidase (Amersham Pharmacia Biotech) was allowed to bind to the major coat protein of M13. After another wash step, the assay was visualized by adding H_2O_2 and ABTS (2′,2′-azino-bis(3-ethylbenzthiazoline-6-sulfonic acid)) (Pierce) followed by quenching with an equal volume of 4 N sulfuric acid. Absorbance at 450 nm was measured as a function of diluted phage using a microplate reader (Bio-Rad).

Peptide Synthesis. Peptides were synthesized at the Oligopeptide Synthesis Facility at the University of Chicago using F-MOC chemistry on an ABI 430A peptide synthesizer. Peptide sequences were verified using mass spectrometry (on an ABI 300 LC/MS) and by peptide sequencing. Peptides were purified using a Vydac 18 column on a Shimadzu HPLC and were judged to be greater than 95% pure.

Determination of Equilibrium Binding Constants. Equilibrium binding constants for S-peptide variants were determined by surface plasmon resonance (SPR) using a BIACORE 2000 instrument (*20*). S-protein (50 μg/mL in 10 mM sodium acetate buffer, pH 4.5) was coupled covalently to a CM5 carboxylated dextran sensor chip using *N*-hydroxysuccinimide (NHS) and *N*-ethyl-*N*′-[(3-dimethylamino)propyl] carbodiimide hydrochloride (EDC) chemistry. This coupling chemistry results in a random distribution of S-protein on the sensor chip with covalent linkages made via primary amines on the protein surface. Uncoupled NHS-ester groups were blocked with 1 M ethanolamine. A low density (approximately 400 RU) and a high density (approximately 1100 RU) of S-protein were coupled to individual flow cells of the sensor chip by this procedure. A third flow cell was NHS/EDC activated and blocked, but contained no coupled S-protein and served as a control surface. Interaction analyses were carried out using at 25 °C in 10 mM HEPES, 150 mM NaCl, 0.005% surfactant P20, pH 7.4, (HBS-P buffer, BIACORE Inc.) by flowing a range of concentrations of a given S-peptide variant across each flow cell (at a rate of 20 μL/min) and measuring the response level (in RUs) as a function of time. For WT S-peptide, concentrations of 30−1000 nM were injected, while 3−100 nM was typically used for the high affinity variants. For weakly binding peptides, concentrations up to 20 μM were injected. Higher concentrations were prohibited by the solubility of the peptide.

Association and dissociation rate constants were determined using BIAevaluation 3.0.2 (BIACORE Inc.) software and binding curves for each set of concentrations were fit simultaneously (a global fit) to a 1:1 (Langmuir) binding model (*20*). Equilibrium binding constants were obtained from the ratio of the kinetic dissociation and association rates. The measured binding constant was found to be independent of the concentration of variant injected as well as the density of S-protein coupled to the surface (data not shown). Errors listed in Table 3 are the standard deviations observed for 5−7 independent experiments, each of which consisted of a global fit to five concentrations of injected peptide. The chi-squared values reported for the fits shown in Figure 3 are for a single experiment but are typical of those observed for WT and the high affinity variants.

Circular Dichroism. CD experiments were conducted using an AVIV Associates 62DS spectrometer. The ellipticity was monitored at a wavelength of 222 nm from 25 to 75 °C at 2° increments using a cell with a 1-mm path length. Equal molar mixtures of a peptide and S-protein were made at 25 μM in 10 mM HEPES, 150 mM NaCl, pH 7.4 and heated at a rate of 1 °C/min with a 1 min equilibration at each temperature. The fraction of unfolded protein was determined from $P_{unf} = (\theta - \theta_F)/(\theta_U - \theta_F)$ where θ_F and θ_U are the mean residue ellipticity values at the fully folded and fully unfolded baselines.

Activity Assay. The activities of peptide:S-protein complexes were determined by following the change in absorbance at 292 nm due to the hydrolysis of cytidine 2′:3′ cyclic monophosphate (cCMP) (*21*). Peptide and S-protein were combined in an equal-molar ratio at a final concentration of 5 μM. RNase A and S-protein were also measured at 5 μM individually. The assay was performed at 25 °C in 50 mM Tris, 150 mM NaCl at pH 7.1. Stock concentrations of cCMP were at 10 mg/mL and were diluted into the cuvette immediately prior to measurement. Absorbance measurements were made at 1 s intervals on an UV spectrophotometer (Hewlett-Packard) using a 1-mL cuvette and a 1-cm path length. Initial velocities were determined from the slope of the initial 30 s of data and were plotted as a function of substrate concentration.

Kinetic Association and Dissociation Constants in GuHCL. The association and dissociation rate constants were measured in GuHCl using SPR. GuHCl solutions (0.0−0.4 M) were freshly prepared in 10 mM HEPES, pH 7.2. NaCl (0.5−0.1 M, respectively) was added to the buffer such that the ionic strength was constant at 0.5 M. In this way, differences in affinity due to changes in ionic strength, osmotic pressure, viscosity or anion binding were minimized. The buffer was filtered (0.2 μ) and degassed for approximately 10 min, and was used for diluting S-peptide variants, as well as for the running buffer in the SPR experiments. Data were collected and analyzed as described above.

Table 2: Clones Isolated from the S-Peptide NNS Library (Top) and the Soft Library (Bottom) after Five Rounds of Sorting[a]

	1	2	3	**4**	**5**	**6**	**7**	8	**9**	**10**	11	12	13	14	15	16	17	18	19
wt	K	E	T	**A**	**A**	A	**K**	F	**E**	**R**	Q	H	M	D	S	S	T	S	A
1	K	E	T	**N**	**W**	A	**W**	F	**W**	**D**	Q	H	M	D	S	S	T	S	A
2	K	E	T	**G**	**W**	A	**L**	F	**V**	**Q**	Q	H	M	D	S	S	T	S	A
3	K	E	T	**V**	**M**	A	**N**	F	**Q**	**M**	Q	H	M	D	S	S	T	S	A
4	K	E	T	**G**	**D**	A	**V**	F	**A**	**R**	Q	H	M	D	S	S	T	S	A
5	K	E	T	**G**	**W**	A	**A**	F	**V**	**K**	Q	H	M	D	S	S	T	S	A
6	K	E	T	**G**	**W**	A	**T**	F	**V**	**E**	Q	H	M	D	S	S	T	S	A
7	K	E	T	**K**	**L**	A	**F**	F	**L**	**K**	Q	H	M	D	S	S	T	S	A
8	K	E	T	**W**	**W**	A	**W**	F	**F**	**G**	Q	H	M	D	S	S	T	S	A
9	K	E	T	**T**	**W**	A	**E**	F	**T**	**W**	Q	H	M	D	S	S	T	S	A
10	K	E	T	**P**	**W**	A	**S**	F	**N**	**K**	Q	H	M	D	S	S	T	S	A
11	K	E	T	**A**	**M**	A	**M**	F	**V**	**T**	Q	H	M	D	S	S	T	S	A
12	K	E	T	**L**	**W**	A	**W**	F	**M**	**W**	Q	H	M	D	S	S	T	S	A
LB1				**G**	**W**		**W**		**V**	**K**									
LB2					**W**		**I**		**V**										

	1	**2**	**3**	**4**	**5**	**6**	**7**	**8**	**9**	**10**	**11**	**12**	**13**	**14**	**15**	**16**	**17**	**18**	**19**
1	F	E	T	A	A	A	I	F	D	R	L	N	M	L	S	S	T	S	M
2	K	I	S	A	S	T	N	F	V	R	E	L	I	D	R	L	T	S	V
3	L	E	T	S	A	A	I	L	E	R	L	R	M	Y	I	T	T	S	A
4	L	A	T	L	A	A	I	F	E	R	R	L	M	D	W	S	N	N	A
5	M	Y	V	V	S	A	I	F	E	R	L	H	M	G	S	S	T	S	A
6	K	D	T	A	N	T	K	L	E	S	Q	Q	M	V	N	S	S	C	A

[a] Positions included in the library are in bold.

Table 3: Kinetic Association and Dissociation Constants for S-Peptide Variants as Determined by Surface Plasmon Resonance

S-peptide variant	$k_{on}\,10^4$ ($M^{-1}\,s^{-1}$)	$k_{off}\,10^{-2}$ (s^{-1})	K_d (nM)
wild type	1.4 (± 0.4)	0.85 (± 0.1)	599.0 (± 68)
LB1	90.0 (± 34)	1.51 (± 0.3)	16.7 (± 3.2)
LB2	104.1 (± 21)	0.56 (± 0.1)	5.4 (± 1.3)
A5W	18.0 (± 1.3)	0.75 (± 0.1)	41.6 (± 5.2)
nonpolar bias (NP)[a]	4.4 (± 0.3)	0.6 (± 0.1)	136 (± 15.1)
polar bias (PP)[b]	ND	ND	>10 000
W5/NP	30.9 (± 8)	0.46 (± 0.1)	14.9 (± 3.0)
W5/NP/E9P	0.022 (± 0.005)	0.19 (± 0.05)	8570 (± 2340)
W5/NP/A6G	ND	ND	>20 000

[a] Sequence changes (NP) A4V, A5M, K7M, E9S, R10F. [b] (PP) A4E, A5E, K7G, E9Q.

RESULTS

Identification of the S-Peptide Binding Epitope. Figure 1 shows the interaction of RNase S-peptide and S-protein (*15*). Residues 3 through 13 form an α-helix when bound to the S-protein. However, circular dichroism measurements of unbound S-peptide in solution show little helical structure, indicating that the peptide must form an α-helix at some point during the binding process. Previous studies have highlighted the importance of several residues for binding, particularly Phe-8 (*22*) and Met-13 (*23*), but no systematic study of the entire interface has been undertaken.

An alanine scan was used to gauge qualitatively the relative importance of each of the first 15 residues of S-peptide using a phage ELISA format. As shown in Figure 2, alanine substitutions for residues Phe-8, Gln-11, Met-13, Asp-14, and Ser-15 significantly affect binding. His-12 also appeared to be important for binding (not shown), but phage titers for this mutant were significantly lower than for the other mutants suggesting the result could be influenced by poor peptide expression. Thr-3 and Lys-7 show moderate decreases in binding, and alanine mutations of residues Glu-2, Glu-9, and Arg-10 have little effect on binding. Residues 4, 5, and 6 are alanine in wild type and were not evaluated. Phe-8 (*22*), Met-13, and Gln-11 have been shown previously to be key contact residues and that replacement with other amino acids typically results in a reduction in affinity (*24*). The ELISA alanine scan clearly identified these residues as important for binding.

Some of the alanine scanning results could not be directly assigned to structural factors. The decrease in binding upon mutation of Thr-3 is apparently an indirect effect, since this residue makes no contact with S-protein (*15*). However, truncation of the N-terminus past residue 3 has been shown to cause a significant decrease in binding (*10*) and may explain why a reduction in affinity is observed in the alanine scan. Since Thr-3 is the first residue of the helical portion of S-peptide, it is possible that this amino acid plays a role in the formation or stabilization of the helical segment. The observed reduction in affinity for S15A may also reflect some type of helix capping effect.

Phage Display Mutagenesis Libraries Using Full Randomization. Full randomization employing the NNS codon strategy was used to introduce combinations of all possible amino acid types at the targeted positions. The residues that were targeted for mutagenesis were selected on the basis of the alanine scan binding data (Figure 2) and structural information (Figure 1). Amino acids known to be important for binding (such as Phe-8 or Met-13) were excluded, as were residues important for catalysis (such as His-12). The S-protein sample obtained from Sigma contained two species, the 21−124 fragment and the 20−124 fragment, as determined by mass spectrometry (data not shown). The 20−124 fragment was the dominant fragment (about 75% in the sample studied), and so the S-peptide construct included residues 1−19. The S-peptide mutagenesis library included positions Ala-4, Ala-5, Lys-7, Glu-9, and Arg-10. Analysis of the crystallographic structure of RNase S (*15*) suggests that position 5 and perhaps position 4 could make contact with S-protein if the wild-type Ala was replaced by a longer

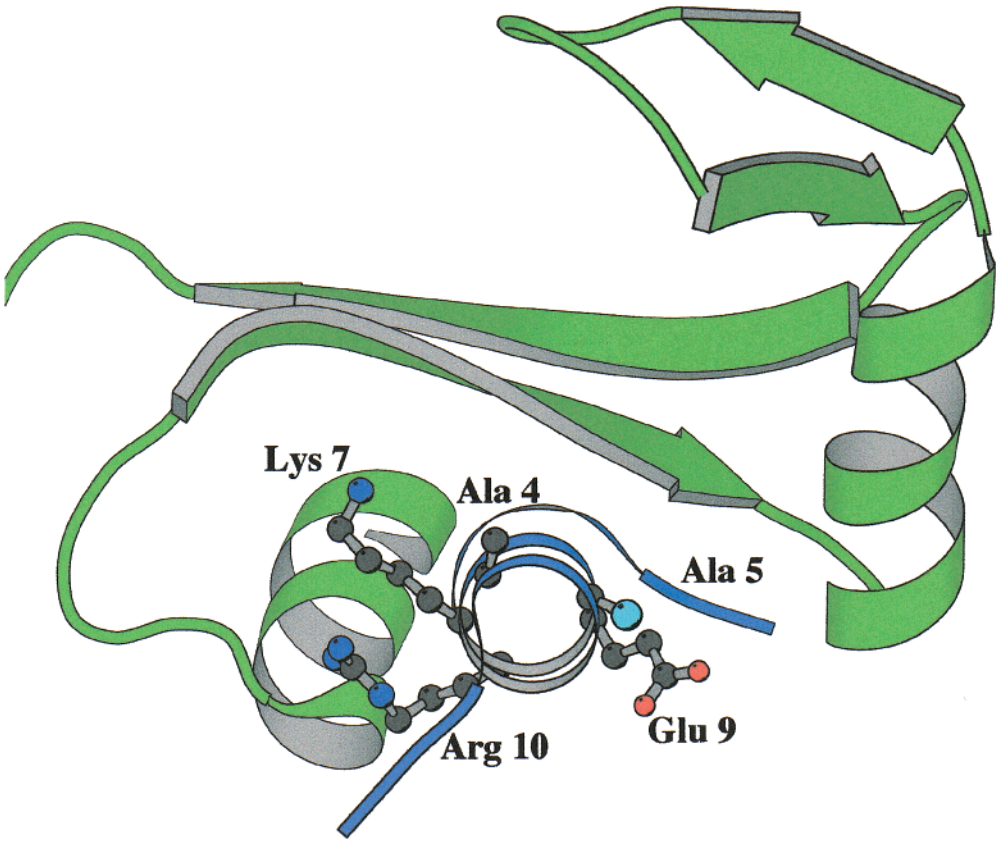

FIGURE 1: The complex between S-peptide (1−15) and S-protein (*15*). S-peptide is shown in blue, and the amino acids included in the library are also indicated. The Cβ atom of the Ala-5 side chain is colored cyan for clarity. This figure was prepared using MolScript (*34*).

side chain. Lys-7, Glu-9, and Arg-10 do not appear to make substantial contributions to binding, as evidenced by the ELISA data, but they do make contacts with S-protein and could perhaps be optimized. Lys-7, for example, is thought to make important contacts with RNA during catalysis, and so this residue has not been optimized by nature for interaction with S-protein.

Gln-11 and Asp-14 were added in subsequent libraries, since the use of "biased" libraries enables additional amino acid positions to be randomized. Gln-11 and Asp-14 were chosen since they appeared to contribute more significantly to binding (Figure 2) and because they are not completely buried in the S-peptide/S-protein complex, suggesting these residues could be optimized. Asp-14 was also of interest due to contacts with His-48 and Arg-33 of S-protein, suggesting possible electrostatic interactions involving this residue.

Enrichment of the phage titer was observed after 3−4 rounds and reached a maximum of about 300-fold over background after six rounds of sorting. Table 2 lists the sequences of clones picked after the sixth round. Residue 5 shows a strong preference for Trp (present in 8 of the 12 sequences) after affinity maturation (Table 2, top). On the basis of the expected frequency of occurrence for this residue, the significance score is 12.7 ($(P_f - P_e)/\sigma_n$). This compares to the other consensus residues that were found to have scores ranging from 2 to 5. Position 4 shows some preference for Gly, and positions 7 and 9 have a preference for hydrophobic groups.

Partial Randomization. A complementary sorting strategy was employed where all 19 residues of S-peptide were partially randomized together using what has been termed a "soft-randomization" (*19*). The resulting library allows for all 20 amino acids at each of the 19 positions, but retains a high percentage (~50%) of wild-type codons in the library. Since the residue types are biased toward the wild-type sequence positions, finding a consensus for a nonwild-type residue at a particular site indicates a potential enhancement.

Modest enrichment of phage titer occurred after two rounds and increased slowly to about 25-fold after 5 rounds. Sequence data for clones obtained using this strategy are also listed in Table 2. As expected, the soft randomization returned wild-type residues at most positions; however, position 7 shows a strong preference for Ile rather than the wild-type Lys (Table 2, bottom). Several positions (Lys-1, Glu-2, His-12, Asp-14, and Ser-15) show little consensus, while Gln-11 exhibits a slight preference for Leu. We note that to identify alternate residue types using this strategy requires sequencing a much larger set of clones to establish the statistical significance of the selected amino acid type. Nevertheless, in this application the dominance of Ile at position 7 suggests that it should be evaluated.

Binding Constant Determination for Consensus Peptides. On the basis of the above sequence information, two peptides were synthesized and their equilibrium binding constants were measured using SPR on a BIACORE 2000 instrument. LB1 contained the consensus residues from the NNS library (A4G, A5W, K7W, E9V, and R10K). LB2 combined the residues from a composite of the full and partial randomized libraries (Table 2). It differs from wild type S-peptide at only three positions (A5W, K7I, and E9V). Figure 3 shows the binding sensorgrams of WT S-peptide and LB2 as determined by SPR. The small dots are the raw data, and the

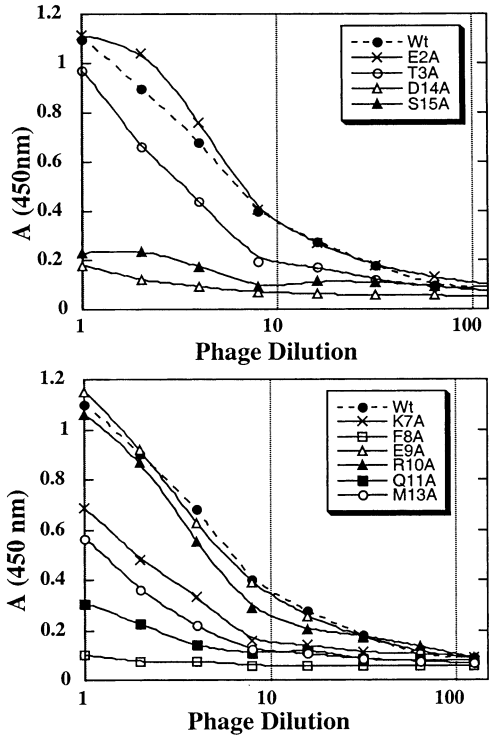

FIGURE 2: Alanine scanning of S-peptide by phage binding ELISA. The absorbance at 450 nm is plotted as a function of phage dilution. The top panel shows the residues at the ends of the binding epitope, and the bottom panel contains residues thought to be most important for binding and catalysis. Amino acids 4, 5, 6, and 16−19 were not evaluated. H12A appeared to have a binding contribution, falling between Q11A and F8A on the bottom panel, but this mutant along with K1A could not be expressed reproducibly on phage and were therefore not included.

solid line is a fit of the data using a 1:1 Langmuir binding model. Table 3 shows the kinetic association and dissociation rates, obtained from these fits, for the phage-optimized variants LB1 and LB2 along with the wild-type S-peptide (residues 1−19).

The affinity of a truncated version of S-peptide (residues 1−15 as measured by calorimetry was found to be 100−300 nM (*16*, *23*). It has been reported that the full length S-peptide binds 2-fold weaker than the truncated version (*10*). While the value of 600 nM determined here is in reasonable agreement with these studies, we note that other studies report much tighter values for the full-length peptide (*11*, *25*−*27*). We believe that part of the discrepancy in the literature values is presumably due to different experimental techniques and buffer conditions, as well as the use of full-length and truncated S-peptides. In this study, our conclusions are based on factors involving the relative changes in binding after affinity maturation. In this regard, our binding analyses are internally consistent as measured by either SPR or CD.

Table 3 shows that the high affinity variants LB1 and LB2 bind 36- and 110-fold more tightly than wild type, respectively. Surprisingly, the majority of this improvement is achieved through an increase in the on-rate. In LB2, the on-rate is 75-fold faster than for the wild-type S-peptide. The off-rates for these variants were all within a factor of 3 of wild type. This is in contrast to other protein systems where affinity enhancements or mutagenesis typically affect off-rates (*1*, *3*). The three mutations in this peptide are hydrophobic; two of which replace the hydrophilic residues

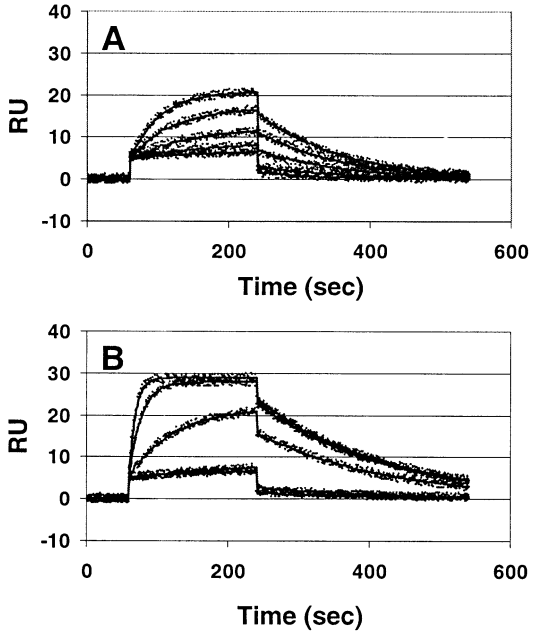

FIGURE 3: Kinetic analysis of (A) WT S-peptide and (B) LB2 binding to immobilized S-protein (1100 RU) using surface plasmon resonance on a Biacore 2000 instrument. Two-fold serial dilutions of each peptide were measured, starting at 1000 nM for WT and 100 nM for LB2. Each set of curves was simultaneously fitted using a 1:1 binding model (solid lines) to obtain k_{on} and k_{off}. Chi-squared values were 0.44 for WT and 0.36 for LB2. The residuals were randomly distributed around the fit within 1 RU.

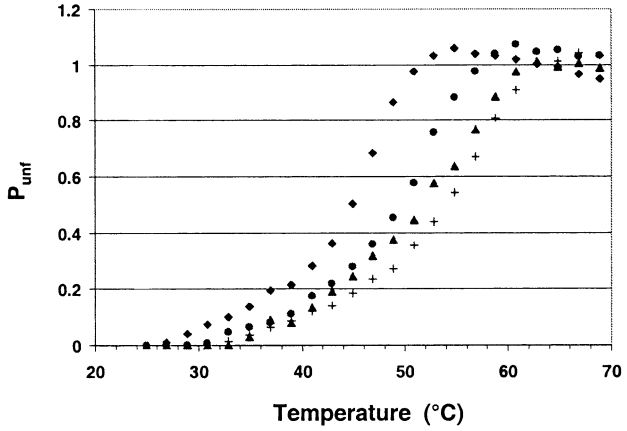

FIGURE 4: Thermal unfolding of peptide/S-protein complexes for wild type (diamonds), A5W (circles), LB1 (triangles), and LB2 (crosses). P_{unf} is the fraction of protein unfolded as determined by circular dichroism at a wavelength of 222 nm.

Lys-7 and Glu-9. This suggests that the tighter binding could be due to an increase in hydrophobic interactions between the S-peptide and the S-protein. Trp-5 appears to be responsible for much of the tighter binding. The A5W mutant alone results in a 14-fold improvement in the affinity, a majority of which is due to its faster on-rate (Table 3).

LB2/S-Protein Complex has Enhanced Thermal Stability. Thermal denaturation experiments were performed on peptide/S-protein complexes to determine how the phage-optimized peptides influence structural stability. Figure 4 shows the thermal transition from folded to unfolded as determined by circular dichroism at 222 nm. The lowest T_m is that of wild-type S-peptide at 44.8 (± 0.4) °C, which is in good agreement with published values of 43−44 °C (*29* and

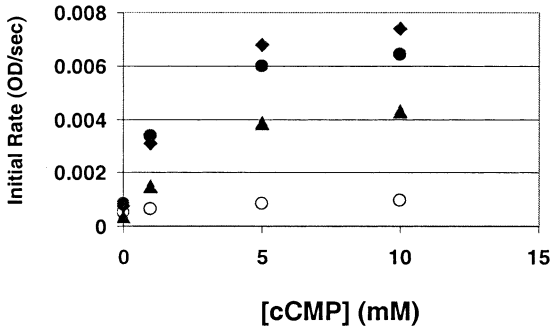

FIGURE 5: Enzymatic activity of RNase A (diamonds), RNase S (filled circles), S-protein (open circles), and the LB2/S-protein complex (triangles) using a cytidine 2′:3′ cyclic monophosphate (cCMP) assay. The absorbance at 292 nm was measured as a function of time after addition of substrate. Initial rates for each concentration of substrate were determined from the slope of the first 30 s of data.

references therein). The LB2/S-protein complex had the highest T_m (53.8 ± 0.4 °C) followed by LB1 (51.6 ± 0.6 °C) and A5W (49.5 ± 0.5 °C). All three peptides greatly enhance the thermal stability of the complex and the observed trend in the T_m values correlates well with the K_d values measured by SPR using the Biacore.

Binding of S-Peptide Variants Is Similar to WT S-Peptide. It was important to establish whether the improvement in affinity in LB2 influenced the energetic contributions of other contact residues in WT S-peptide. This might be the case if the mode of binding was functionally different than that of wild type. An alanine scan was performed on LB2 using the same ELISA format as was used for wild type. It was found that contributions by other residues comprising LB2 were generally similar to that of wild-type S-peptide (data not shown), suggesting that the importance of these residues was retained in the phage optimized peptides. The LB2/S-protein complex was also assayed for enzymatic activity using cyclic cytidine-2′:3′-monophosphate as a substrate (*21*) and was found to retain significant activity as compared to wild type RNase S (Figure 5). Taken together, it appears that the high affinity variant, LB2, binds in a structurally similar manner as the wild-type peptide. Furthermore, the changes that brought about the high affinity appear to add additional "hot spots" and do not significantly alter the contributions by the rest of the binding epitope.

Phage Display Mutagenesis Using Polar and Nonpolar Biased Libraries. On the basis of the distinct correlation between binding strength and the hydrophobic character of the altered residues, the strong preference for hydrophobic residues in high-affinity variants was investigated using "biased" phage display libraries. Two biased phage display libraries were constructed (*17*). These libraries were designed to allow only a subset of polar (VRS wobble code, see Table 1) or nonpolar (NYS code) residues at the targeted sites. We note that the NYS nonpolar library does not contain Trp, so that S-peptide was being optimized without the benefit of the amino acid that indicated the highest consensus in the NNS library and made the strongest contribution to binding.

After five rounds of sorting of the nonpolar biased library an approximately 200-fold enrichment in phage titer was observed. Only a 25- to 50- fold enrichment over background was achieved in a similar sorting of the polar biased library. Figure 6 shows the consensus selection for clones obtained

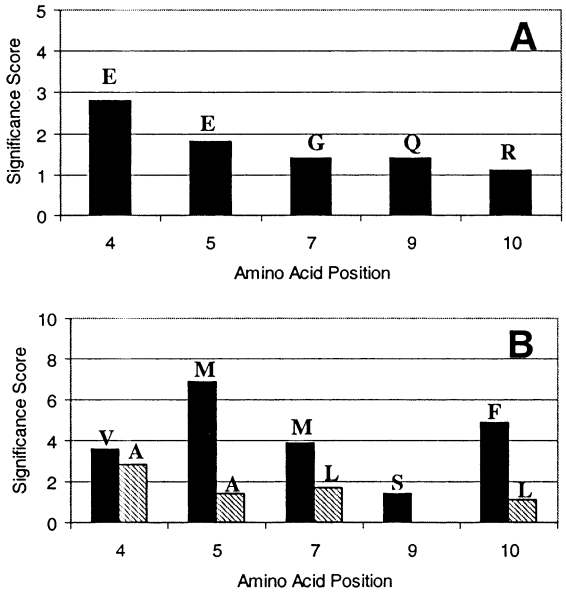

FIGURE 6: Consensus residues for the polar biased library (A) and nonpolar biased library (B) after five rounds of sorting. The ratio $(P_f - P_e)/\sigma$ represents the frequency of occurrence of a particular residue and is described more fully in Experimental Procedures. Ratios below 1.5 were not shown. The number of clones sequenced, *n*, was 16 for the polar and 22 for the nonpolar library.

after the fifth round. The low significance scores for the polar sequence indicates that there is little specific selection within the library (Table 6).

Peptides corresponding to the consensus sequence from each library (denoted nonpolar and polar bias in Table 3) were synthesized, and the equilibrium binding constants were determined by SPR analysis. The nonpolar consensus variant (A4V, A5M, K7M, E9S, R10F) produced from the NYS library resulted in 4.4-fold tighter binding as compared to wild-type S-peptide. This increase in binding was reflected mostly in a 3-fold increase in the on-rate. The polar variant (A4E, A5E, K7G, E9Q) showed no detectable binding when concentrations as high as 10 μM were injected. The lack of any consensus residues and the very poor affinity indicate that sets of polar residues at positions 4, 5, 7, and 9 cannot provide a productive interface to the S-protein. This is consistent with the NNS randomization where very few polar residues were observed for these residues.

Trp 5 Is Important for High Affinity. The NYS nonpolar biased library improved S-peptide binding, but 8-fold less than the consensus residues determined from the NNS library (Table 3). Although the NYS library codes for nine mostly hydrophobic amino acids, it does not contain Trp. With consideration of the potential importance of a Trp at position 5, a biased phage display library was constructed that used the TNS codon at position 5. The number of amino acids present at this position is smaller than for the NYS codon but contains Trp (Table 1). For positions 4, 7, 9, 10, 11, and 14, the larger NYS library was used. We note that the use of biased libraries reduces the number of possible codon combinations, and so the randomization of more residues did not compromise the completeness of the library (*17*).

After five rounds of sorting, Trp and, to a lesser degree, Phe were selected at position 5 (Figure 7). A Met at residue 7 is strongly selected, which is consistent with the previous NYS library (Figure 6, lower panel). Unexpectedly, Pro

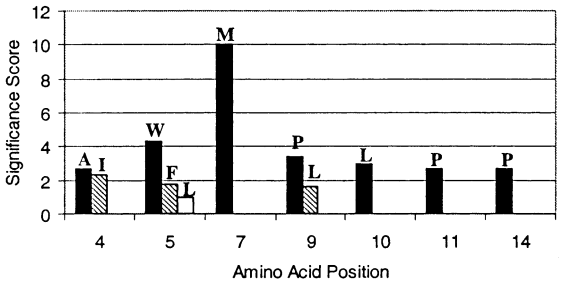

FIGURE 7: Consensus residues for the nonpolar library where the TNS codon strategy was used for position 5. The *y*-axis is described in Figure 6, and *n* was equal to 14.

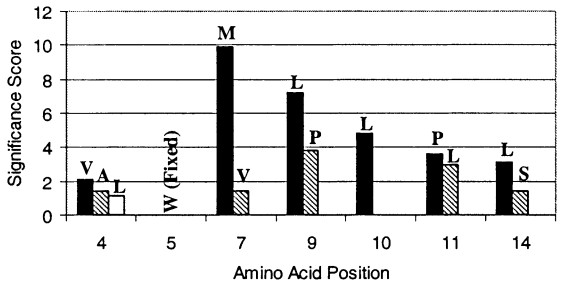

FIGURE 8: Consensus residues for the nonpolar library where Ala5 was mutated to Trp. The *y*-axis is described in Figure 6, and *n* was equal to 17.

appeared at positions 9, 11, and 14, although in no case was it strongly selected. An additional library was constructed in which Ala-5 was changed to Trp with the other residues (4, 7, 9, 10, 11, and 14) randomized with the nonpolar NYS codons. Figure 8 shows that at positions 9 and 11 prolines were selected again.

To investigate the unexpected selection of Pro in the middle of the α-helical segment, two peptides were synthesized based on the sorting results. One peptide (W5/NP/E9P) contained mutations A5W, K7M, E9P, and R10L, while the other peptide (W5/NP) contained A5W, K7M, E9V, and R10L. The binding data shown in Table 3 indicate that the W5/NP peptide binds 40-fold more tightly than wild-type S-peptide. The introduction of the Pro residue at residue 9 (W5/NP/E9P) results in a binding constant 14-fold weaker than wild-type S-peptide. Thus, in the context of this peptide, a Pro at position 9 decreases binding by about 550-fold. The loss of binding affinity is primarily a result of a more than 60-fold decrease in the on-rate. This would be expected for a mutation that hindered the ability of S-peptide to form an α-helix, but since position 9 was one of the three mutated amino acids in the high affinity LB2 variant, we cannot rule out a destabilizing contribution due to the loss of a contact residue.

To clarify whether the reduction in binding affinity in the W5/NP/E9P mutant was mainly a result of the Pro affecting the helical character of the peptide another peptide was synthesized. In this peptide, Pro-9 of W5/NP/E9P was reverted to the wild-type Glu, and position 6 was changed to a Gly (W5/NP/A6G). Residue 6 makes no contact with S-protein, and so replacement by Gly should primarily affect helix stability. Table 3 shows that this replacement is also very destabilizing, with no detectable binding at peptide concentrations as high as 20 μM. It appears that the Gly and Pro substitutions have a deleterious affect on helix formation, as expected. Therefore, it seems that the appearance of Pro in the phage optimized sequences is a consequence of the high affinity afforded by the A5W mutation which makes marginally stable peptide variants out of otherwise destabilizing changes. The reason Pro was slightly enriched at these positions is unclear.

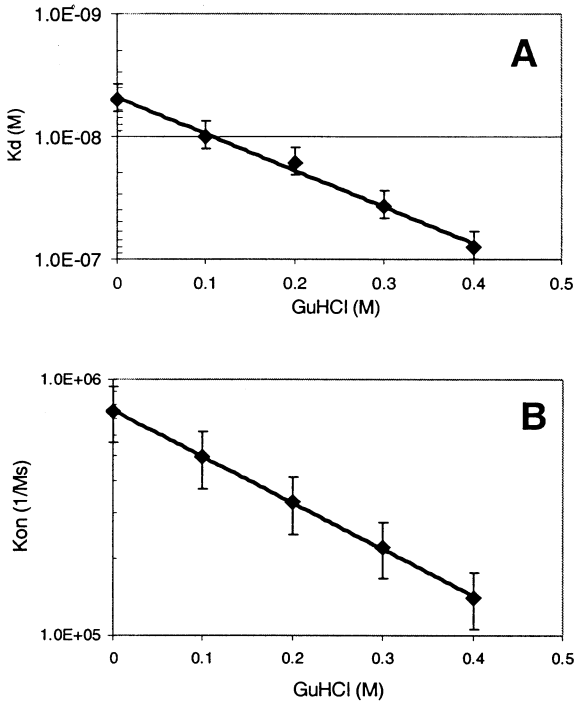

FIGURE 9: Sensitivity of the equilibrium binding constant (A) and the kinetic association rate (B) of the high affinity S-peptide variant LB2 to GuHCl as measured by surface plasmon resonance (SPR). Linear plots were also obtained for wild-type S-peptide (not shown). The m-values reported in Table 4 were determined by fitting these data to eq 2.

Effect of GuHCl on Kinetic Parameters. Although it is likely that Gly and Pro affect the on-rate by disrupting helix formation, the mechanism by which Trp-5 affects k_{on} is not obvious. One possibility is that the hydrophobic changes in LB2 stabilize the transition state (*12*). To explore this possibility, the effect of GuHCl on the equilibrium binding constant and the kinetic association rate was measured for WT (not shown) and the affinity matured LB2 variant (Figure 9) using various concentrations of denaturant. The slope (or m-value) of this plot gives a measure of the sensitivity of these constants, which can then be used to determine the effect of mutations on the folding process. The m-values were determined by fitting the data to (*11*)

$$k = k_o \exp(m^{\ddagger}/RT[\text{GuHCl}]) \qquad (2)$$

Where k and k_o are the equilibrium or kinetic rate constants in the presence or absence of denaturant, and $m^{\ddagger}$ is the slope (or m-value) for that parameter in the presence of denaturant. The ionic strength dependent term was set equal to zero since the measurements presented here were made under conditions of high (and constant) ionic strength (see ref *11*). The m-values obtained from the fits are reported in Table 4. The ratio of $m^{\ddagger}(k_{on})/m^{\ddagger}(K_{eq})$ has been shown to provide a measure of the percentage of buried surface area in the transition state relative to the total buried surface area of the complex (*12*, *33*). It was found that a greater percentage of surface area is

Table 4: Effect of GuHCl on the Association Rate and Equilibrium Binding Constant for WT S-peptide and Affinity Matured Variants

	WT	LB2
$m^{\ddagger}$ (k_{on}) kcal mol^{-1} M^{-1}	−1.9	−2.5
$m^{\ddagger}$ (K_{eq}) kcal mol^{-1} M^{-1}	3.3	3.2
percent buried[a]	59%	77%

[a] The percent buried is determined from the ratio of -$m^{\ddagger}$(k_{on}) /$m^{\ddagger}$(K_{eq}) and is a measure of the percentage of buried surface area in the transition state relative to the total buried surface area of the complex (*12*, *33*).

buried in the transition state for LB2 (77%) as compared to WT (59%).

DISCUSSION

Phage display mutagenesis has produced several variants of S-peptide that bind to S-protein significantly more tightly than wild-type S-peptide. The tightest binding variant, LB2, has a binding constant of 5.4 nM, which is more than 100-fold tighter than wild-type S-peptide. The midpoint of the thermal denaturation of the LB2/S-protein is 9°C higher than WT/S-protein, indicating that the complex with LB2 has enhanced stability. The improvement in binding affinity is brought about by just three residues and is dominated by the A5W mutation. When the tryptophan is not included in the selection process (as in the polar and nonpolar biased libraries), only modest improvements in binding affinity could be achieved.

The single Ala → Trp mutation at position 5 increases the binding affinity of the peptide by almost 15-fold. Interestingly, the alanine scan of LB2 indicated relatively small effects for the other two changes at positions 7 and 9. This suggests that the full binding capacity of the peptide (110-fold over wild type) is not based on additivity. Further studies, as well as detailed crystallographic information, will be required to explain fully the origin of the enhanced affinity.

On the basis of the nearly exclusive requirement for Trp at position 5, it appears that a novel "hot spot" has been generated into the S-peptide/S-protein interface. In other examples, it has been shown that Trp residues are common at energetic "hot spots" of protein−protein interfaces (*28*), in part because of the large hydrophobic nature of the side chain. However, the observed effect of interchanging a small hydrophobic side chain (Ala-5) with tryptophan was unexpected.

At other positions, the nonpolar-biased libraries produced consensus residues that were significantly different from those obtained by the more traditional NNS codon strategy. There was, however, good agreement between the three separate phage sorting experiments using this library, indicating that this alternative solution is likely representing a unique solution within the context of the nonpolar biased library. The use of the biased phage display libraries clearly illustrates the nearly singular importance of the Trp at position 5.

A recent study used phage display to discover a 15-mer peptide (termed S15p) that bound to S-protein more tightly (K_d = 105 nM) than S-peptide (*29*). Although S15p had some sequence similarities to S-peptide, including Phe-8 and His-12, the peptide was not catalytically active, in contrast to the LB2 peptide described here. Interestingly, an alignment of S15p with S-peptide indicated that Trp was found at position 5, as well as a hydrophobic Leu at position 9 (*29*). This suggests that phage display of a completely random sequence had found a similar, high affinity solution to that of our more directed approach. It also further emphasizes the importance of Trp-5 in high affinity variants of S-peptide.

Mechanism of Binding. The binding of the wild type and any S-peptide variant consists of two events: folding and recognition. The formation of the S-peptide α-helix in the complex is required to bring the appropriate catalytic elements together to produce a functional RNase S enzyme. Since S-peptide is less than 10% α-helix in the absence of S-protein (*27*), a folding event must occur in conjunction with binding.

Recent studies have attempted to determine whether the α-helix forms prior to binding or if specific interactions between S-protein and S-peptide nucleate the folding of the remaining residues (*13*, *30*, *31*). There is evidence that the transition state between bound and unbound S-peptide is stabilized by hydrophobic interactions, particularly between Phe-8 and S-protein (*12*). Additionally, there is evidence that stabilization of the α-helical conformation, either in the transition state (*12*, *13*) or in the unbound state (*32*) can lead to an enhancement in binding.

The high affinity variants of S-peptide reported here probably derive their improvement from either direct interaction with S-protein or by stabilization of the α-helix. On the basis of modeling studies, it appears that Trp-5 is likely to make significant contact with the S-protein surface without requiring any substantial changes in the protein structure. The accessible surface area of Ala-5 decreases when complexed with S-protein (*15*) and replacement of Trp-5 with the tryptophan derivative, kynurenine, results in fluorescence spectra that suggest this residue interacts with S-protein, but still retains a moderate degree of solvent exposure (J. Dwyer, S. Rajagopal, A. Kossiakoff, unpublished data). Efforts to crystallize complexes containing these high affinity variants are currently underway.

Characteristics of the LB2 S-Peptide Variant. The data in Table 3 indicate that the majority of the increased binding in the phage optimized peptides is achieved by a large increase in the on-rate. This is in contrast to larger systems, such as human growth hormone, where mutations typically only affect the off-rate values (*3*). A recent review (*1*) has suggested that changes in on-rates might be associated with conformational changes in conjunction with binding or to specific interactions that tend to accelerate complex formation.

While the phage display optimization could potentially stabilize the helical conformation of the S-peptide variants at equilibrium, circular dichroism measurements on the LB2 variant at 25 °C are very similar to wild type (data not shown). This suggests that there is no significant increase in the helical population in solution. Furthermore, the helical propensities of the mutated residues are not significantly different from wild type. We note, however, that formation of an α-helical structure is clearly important for binding as demonstrated by the dramatic decrease in binding affinity for the S-peptide variants containing E9P and A6G.

Effects of Increased Hydrophobic Interactions in LB2. It has been suggested that hydrophobic interactions between S-peptide and S-protein stabilize the transition state (*12*) and that 55% of the total buried surface area of the RNase S

complex is also buried in the transition state (*11*). To estimate this value for the high affinity LB2 variant, the kinetic rate constants of WT and LB2 were measured in the presence of GuHCl (Figure 9).

The surface area buried in the transition state can be estimated from the sensitivity of the on-rate to denaturant as compared to the sensitivity of the equilibrium constant (*33*). The sensitivity is gauged through a quantity known as the m-value, obtained by using eq 2 to fit the data shown in Figure 9. On the basis of this analysis, the measured value of 59% for wild-type S-peptide (Table 4) compares very well to the value of 57% obtained by stopped-flow experiments for the binding of an S-peptide variant in GuHCl (*11*). The m-values obtained from the sensitivity of k_{on} for this variant ($m_{on} = -1.6$ kcal mol^{-1} M^{-1}) (*11*) also compare favorably to those measured here for wild type. The on-rate for LB2 is more sensitive to denaturant, and we estimate that nearly 77% of the final buried surface area is buried in the transition state (Table 4). Since the Trp side chain is about 146 Å^3 larger than the alanine side chain, there would be an increase in the total buried surface area for LB2 as compared to wild type. The kinetic measurements in GuHCl suggest that the additional hydrophobic surface area in Trp-5 may also be stabilizing the transition state. Stopped-flow experiments on these peptides, which will allow binding measurements to be made on a much faster time scale, will certainly help clarify the role of Trp in the folding and recognition process.

Conclusions. Many different effects, including the interactions between specific side chains and structural rearrangements govern affinity maturation by phage display. Understanding the relative importance of these contributions is likely to be difficult in a large macromolecular interface. In this paper, we have used RNase S to explore the characteristics of the affinity-matured interface between a high affinity S-peptide variant and S-protein. The results presented here indicate that increased hydrophobic interactions between S-peptide and S-protein, mediated though Trp-5, make a significant contribution to the improvement in binding. The use of biased libraries has been shown to generate alternative, unique solutions that would not have been obvious from a traditional NNS phage display mutagenesis library. This fact, coupled with the greater number of residues that can be randomized in a single library, suggest that biased libraries may prove to be useful in controlling the directed evolution of macromolecular interfaces.

ACKNOWLEDGMENT

We thank Mark Dennis of Genentech, Inc. for assistance in making the initial phage display construct, Henry Lowman and Sachev Sidhu of Genentech for helpful discussions on phage display, Tobin Sosnick of the University of Chicago for suggesting the m-value experiments, and Mary Kay Delmedico of Trimeris, Inc. for access to a CD spectrometer.

REFERENCES

1. Stites, W. E. (1997) *Chem. Rev. 97*, 1233−1250.
2. Clackson, T., and Wells, J. A. (1995) *Science 267*, 383−386.
3. Cunningham, B. C., and Wells, J. A. (1993) *J. Mol. Biol. 234*, 554−563.
4. Jin, L., Fendly, B. M., and Wells, J. A. (1992) *J. Mol. Biol. 226*, 851−865.
5. Novotny, J., Bruccoleri, R. E., and Saul, F. A. (1989) *Biochemistry 28*, 4735−4749.
6. Kossiakoff, A. A., Somers, W., Ultsch, M., Andow, K., Muller, Y. A., and de Vos, A. M. (1994) *Protein Sci. 3*, 1697−1705.
7. Lowman, H. B. (1997) *Annu. Rev. Biophys. Biomol. Struct. 26*, 401−424.
8. O'Neil, K. T., and Hoess, R. H. (1995) *Curr. Opin. Struct. Biol. 5*, 443−449.
9. Lowman, H. B., and Wells, J. A. (1991) *Methods Comput. Methods Enzymol. 3*, 205−216.
10. Levit S., and Berger, A. (1975) *J. Biol. Chem. 251*, 1333−1339.
11. Goldberg, J. M., and Baldwin, R. L. (1998) *Biochemistry 37*, 2546−2555.
12. Goldberg, J. M., and Baldwin, R. L. (1998) *Biochemistry 37*, 2556−2565.
13. Goldberg, J. M., and Baldwin, R. L. (1999) *Proc. Natl. Acad. Sci. U.S.A. 96*, 2019−2024.
14. Jackson, D. Y., Burnier, J., Quan, C., Stanley, M., Tom, J., and Wells, J. A. (1994) *Science 266*, 243−247.
15. Kim, E. E., Varadarajan, R., Wyckoff, H. W., and Richards, F. M. (1992) *Biochemistry 31*, 12304−12314.
16. Varadarajan, R., and Richards, F. M. (1992) *Biochemistry 31*, 12315−12327.
17. Dwyer, M. A., Lu, W., Dwyer, J. J., and Kossiakoff, A. A. (2000) *Chem. Biol. 7*, 263−274.
18. Lowman, H. B., and Wells, J. A. (1993) *J. Mol. Biol. 234*, 564−578.
19. Fairbrother, W. J., Liu, J., Pisacane, P. I., Sliwkowski, M. X., and Palmer, A. G. (1998) *J. Mol. Biol. 279*, 1149−1161.
20. Karlsson, R., and Fält, A. (1997) *J. Immunol. Methods 200*, 121−133.
21. Crook, E. M., Mathias, A. P., and Rabin, B. R. (1960) *Biochem. J. 74*, 234−238
22. Filippi, B., Borin, G., and Marchiori F. (1976) *J. Mol. Biol. 106*, 315−324.
23. Connelly, P. R., Varadarajan, R., Sturtevant, J. M., and Richards, F. M. (1990) *Biochemistry 29*, 6108−6114.
24. Filippi, B., Chessa, G., and Borin, G. (1981) *J. Mol. Biol. 147*, 597−600.
25. Graziano, G., Catanzano, F., Giancola, C., and Barone, G. (1996) *Biochemistry 35*, 13386-13392.
26. Schreier, A. A., and Baldwin, R. L. (1977) *Biochemistry 16*, 4203−4209.
27. Hearn, R. P., Richards, F. M., Sturtevant, J. M., and Watt, G. D. (1971) *Biochemistry 10*, 806−817.
28. Bogan, A. A., and Thorn, K. S. (1998) *J. Mol. Biol. 280*, 1−9.
29. Chakravarty, S., Mitra, N., Queitsch, I., Surolia, A., Varadarajan, R., and Dubel, S. (2000) *FEBS Lett. 476*, 296−300.
30. Myers, J. K., and Oas, T. G. (1999) *J. Mol. Biol. 289*, 205−209.
31. Moran, L. B., Schneider, J. P., Kentsis, A., Reddy, G. A., and Sosnick, T. R. (1999) *Proc. Natl. Acad. Sci. U.S.A. 96*, 10699−10704.
32. Mitchinson, C., and Baldwin, R. L. (1986) *Proteins: Struct. Funct. Genet. 1*, 23−33.
33. Schellman, J. A. (1978) *Biopolymers 17*, 1305−1322.
34. Kraulis, P. J. (1991) *J. Appl. Crystallogr. 24*, 946−950.

BI011703B